Original Article
Positron emission tomography objective parameters for assessment of left ventricular assist device infection using ^{18}F-FDG PET/CT

Saul N Friedman[1,2], Maryam Mahmood[3], Jennifer R Geske[4], Muhammad Rizwan Sohail[3,5,6], Geoffrey B Johnson[1,7], John M Stulak[8], Ayse Tuba Kendi[1]

[1]Department of Radiology, Mayo Clinic College of Medicine and Science, Rochester, MN, USA; [2]Division of Nuclear Medicine, Mallinckrodt Institute of Radiology, Washington University School of Medicine, Saint Louis, MO, USA; [3]Division of Infectious Disease, Department of Medicine, Mayo Clinic College of Medicine and Science, Rochester, MN, USA; [4]Department of Biomedical Statistics and Informatics, Mayo Clinic College of Medicine and Science, Rochester, MN, USA; [5]Department of Cardiovascular Medicine, Mayo Clinic College of Medicine and Science, Rochester, MN, USA; [6]Section of Infectious Diseases, Baylor College of Medicine, Houston, TX, USA; [7]Department of Immunology, Mayo Clinic College of Medicine and Science, Rochester, MN, USA; [8]Department of Cardiovascular Surgery, Mayo Clinic College of Medicine and Science, Rochester, MN, USA

Abstract: Left ventricular assist device (LVAD) is a life-saving therapy, but it poses a substantial infection risk. Current evaluation of LVAD infection with ^{18}F-FDG PET/CT is predominately subjective. We present qualitative and semi-quantitative ^{18}F-FDG PET/CT parameters for early detection of LVAD infection and site localization. We retrospectively reviewed all 25 LVAD patients at our institution who had undergone ^{18}F-FDG PET/CT imaging between 2014 and 2018. LVADs were subdivided into five assessed regions: driveline exit site, subcutaneous driveline, LVAD pump, LVAD inflow, and LVAD outflow cannulae. Ultimate diagnosis of LVAD infection was determined by a multidisciplinary primary care team. Qualitative and semi-quantitative analysis of PET/CT data were performed, including calculation of the standardized uptake value maximum, mean, and peak (SUV_{max}, SUV_{mean}, and SUV_{peak}, respectively), as well as metabolic tumor volume (MTV), and total lesion glycolysis (TLG). A total of 14 patients presented with symptoms of infection, and LVAD infection was ultimately diagnosed in 19 of the 25 cases. All cases were correctly identified on ^{18}F-FDG PET/CT with no false positive and no false negative cases, corresponding to a sensitivity and specificity of 100%. The mean SUV_{max} range at noninfected sites was 2.5-3.4, and the range was 5.7-8.1 at infected sites, resulting in a significant difference ($P < 0.01$) at all LVAD regions. ^{18}F-FDG PET/CT is a useful adjunctive tool for assessment of LVAD infection and infection localization, which is crucial for clinical management. A cut-off SUV_{max} 5 is recommended to help diagnose LVAD infection.

Keywords: FDG, PET, infection, LVAD, MCSD, cardiac

Introduction

Heart failure is a major cause of morbidity and mortality in the United States affecting approximately 6.2 million people, and the lifetime risk of heart failure at age 45 through 95 years is 20-45% [1]. Mechanical circulatory support devices (MCSDs) are a life-saving therapy in refractory heart failure, and play an expanding role as a bridge to transplantation or destination therapy for those not eligible for transplantation. The Interagency Registry for Mechanically Assisted Circulatory Support (INTERMACS)

reported enrollment of approximately 23,000 patients from more than 180 hospitals by the end of 2016 [2].

Ventricular assist device (VAD) and, in particular, left ventricular assist device (LVAD) is an important type of MSCD. The basic components of an LVAD are illustrated in **Figure 1**. A percutaneous driveline connects the internal pump to external battery packs. The pump connects the left ventricle to the aorta through cannulae. The percutaneous driveline results in a substantial risk of infection, and incidence rates of
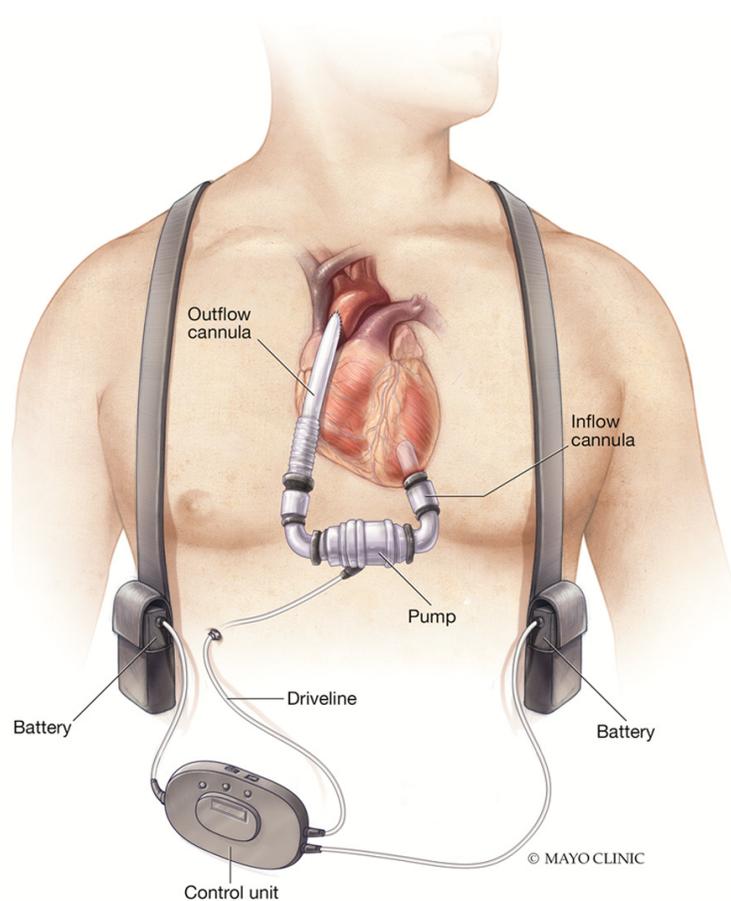
Figure 1. The basic components of a continuous-flow left ventricular assist device (LVAD) include external battery packs connected to the internal pump via a percutaneous driveline. An inflow cannula connects the left ventricle to the pump, which transports blood into the aorta via an outflow cannula.

ve-based cutoff value of 9 cm^3 resulting in a sensitivity of 96%, specificity of 87.5%, PPV of 88.5%, and NPV of 95.5% [14]. de Vaugelade *et al.* evaluated 15 patients with VAD-specific infections and used an ROC curve-based cutoff SUV$_{max}$ of 4.5 resulting in accuracy of 87.5%, sensitivity of 90%, specificity of 66.7%, PPV of 95%, and NPV of 50% [10]. Dell'Aquila and coauthors evaluated 47 patients and report sensitivity of 90.0%, specificity of 71.4%, PPV of 85.71%, and NPV of 78.94%, and discuss SUV$_{max}$ cutoffs ranging from 3.93-5.95 depending on suspected infection location [16].

Given the small sample sizes evaluated within the literature, accurate guidelines for quantitative ^{18}F-FDG PET/CT remain elusive. Our goal is to further develop semi-quantitative parameters for ^{18}F-FDG PET/CT evaluation of potential LVAD-specific infection, while providing additional much needed subject data to the limited available within published literature.

20-50% have been reported [2-6]. Infection is the most common adverse event following MCSD implantation; one third of these infectious complications are VAD-related or VAD-specific [2, 6].

Leucocyte-labeled scintigraphy has been used to evaluate for infection [7-10], but has significantly ($P < 0.01$) lower sensitivity compared to ^{18}F-FDG PET/CT [10, 11]. Several groups have published on the role of ^{18}F-FDG PET/CT [10, 12-18] in LVAD-specific infection evaluation. Avramovic and colleagues reported on 24 patients with VAD-specific infections using an ROC curve-based SUV$_{max}$ cutoff of 6.9, resulting in a sensitivity of 87.5%, specificity of 87.5%, positive predictive value (PPV) of 87.5%, and negative predictive value (NPV) of 87.5%; however, they ultimately concluded that metabolic volume is a better marker with an ROC cur-

Materials and methods

Patients

After institutional review board approval was obtained, a single-center retrospective study was performed on all patients with an LVAD who had undergone ^{18}F-FDG PET/CT imaging between January 1st 2014 and December 31st 2018, independent of original indication for imaging. Written informed consent from all subjects was not necessary as patient data was de-identified and use of the data poses minimal risk to the patients.

^{18}F-FDG PET/CT protocol

Images were acquired using GE Discovery systems (General Electric Medical Systems, GE-MS, Milwaukee, WI) with patients randomly be-

ing assigned to a 690, 710, RX, or MI scanner depending on scanner availability at the time of the study. A single patient was scanned at a sister site on a Siemens Biograph 40 (Siemens Medical Solutions, Knoxville, TN). Patient preparation and scanning protocol was based on Society of Nuclear Medicine guidelines. Patients were instructed to fast at least 4 hours prior to the study, and injected with a standard dose of 0.56 GBq (15 mCi) +/- 10%. Patients then rested for 60-70 minutes during uptake, seated or recumbent in a quiet waiting room with dim lighting to minimize extraneous physiological uptake due to muscles and brown fat.

Myocardial-suppressive low-carbohydrate/high-fat diet was not prescribed for all patients due to the retrospective nature of this study, and the oncologic indication for many of the examinations. A chart review confirmed 3 of the 25 patients adhered to a myocardial-suppressive diet.

Image analysis

Reconstructed PET/CT images were evaluated on a MIMvista workstation (MIM Sofware Inc. Version 6.8.3, Cleveland, OH). PET and fused PET/CT images were reviewed in multiple planes. All studies were first read by a certified nuclear radiologist assigned to the clinical study on the day of acquisition as part of normal institutional workflow. These readers had access to clinical information within the medical record at the time of the study, but were blinded to the infection status of the LVAD as a final diagnosis was not yet possible. The studies were reevaluated by one of the authors with specialized Nuclear Radiology training who was blind to the clinical data but not to the original imaging study interpretation. When discrepancies between the reevaluation and initial interpretation arose, the study was evaluated by a third Nuclear Radiologist reader, who was similarly blinded to the clinical data but not original interpretation, and a final consensus determined. PET reconstruction data without CT attenuation corrections was not archived and therefore not available for the subsequent reevaluation.

LVADs were subdivided into five regions that were assessed separately: driveline exit site, driveline within the subcutaneous tissues, LVAD pump, LVAD inflow, and LVAD outflow cannula.

The standardized uptake value (SUV), a semi-quantitative measure of the normalized concentration of radioactivity in a volume of interest (VOI), was evaluated first and used as a surrogate marker for metabolism similar to multiple prior groups [10, 12-16]. Standardized uptake value maximum (SUV_{max}) is the most commonly used PET parameter and was first evaluated.

Assessments of infection made by the Nuclear Radiologists are based on a combination of SUV and distribution in conjunction with anatomic information from the correlating CT data. No cut-off values were used in the decision process.

If infection was suspected in a region, both qualitative and semi-quantitative analysis of ^{18}F-FDG PET/CT data was performed based on volumes of interest analysis corresponding to volumes of hypermetabolic activity determined using a gradient technique within MIM (PET-edge; MIM Software, Inc., Cleveland, OH) in a semi-automated fashion, similar to prior analyses and described in more depth elsewhere [19]. Standardized uptake value mean and peak (SUV_{mean} and SUV_{peak}, respectively), as well as metabolic tumor volume (MTV), and total lesion glycolysis (TLG) were then calculated from the volumes of interest.

Semi-quantitative SUV_{max}, SUV_{mean}, SUV_{peak}, MTV, and TLG cannot be calculated when an infection is not suspected, as the values are dependent on VOI size and positioning. Without a region of infection, VOI size and positioning would have be randomly chosen and non-reproducible.

Statistical analysis

Clinical and demographic characteristics are presented using descriptive statistics. Comparisons of SUV_{max} at infected and non-infected sites were conducted using nonparametric Wilcoxon rank sum tests, and overall discrimination of SUV_{max} at each site is summarized with receiver operating characteristic (ROC) curves. Dichotomous site-specific SUV_{max} cut-off were established using the value that maximized the area under the curve (AUC). Analyses were conducted using SAS (version 9.4; Cary, NC).

Table 1. Demographics of the included 25 patients (22 male:3 female), 14 of whom had clinical symptoms of infection, and 6 of whom died from infection

	Mean	Standard Deviation	Range
Age (years)	54	14	39-83
BMI	30	5	20-40
Days of symptoms prior to PET/CT[1]	26	35	2-132
Days of antibiotic treatment prior to PET/CT[1]	20	24	2-77
Days from initial presentation to death[2]	206	189	33-544

[1]Based on 14 patients with clinical symptoms of infection. [2]Based on mortality of 6 due to LVAD-specific/related infection.

Table 2. LVAD infection findings based on ^{18}F-FDG PET/CT studies. Final diagnoses were based on a combination of clinical presentation, imaging, and driveline exit, blood, and/or explanted LVAD cultures

Imaging diagnosis	LVAD infection status		Total
	Infection	No infection	
Infection	19	0	19
No infection	0	6	6
Total	19	6	25

Clinical diagnosis

The ultimate diagnosis of LVAD infection was determined based on a combination of clinical presentation, local examination of LVAD components when possible, infectious/inflammatory biomarkers, imaging, and driveline exit, blood, and/or explanted LVAD cultures. The diagnosis was made by the clinical team with expertise in infectious disease and LVADs. Histology correlation was not available and could not be obtained for the patients due to the retrospective nature of this study.

Results

A total of 25 patients (22 male:3 female) were included in the study, and no patients were excluded. All patients were fitted with a continuous flow LVAD, 14 of which were destination therapy while 11 were bridge therapy for intended heart transplant. Additional data are summarized in **Table 1**.

There was a high overall diagnostic accuracy of PET/CT for diagnosis of VAD infections with sensitivity of 100% and specificity of 100%, which is summarized in **Table 2**. The authors only disagreed with the original interpretation on a single study. The original report indicated that LVAD activity was likely inflammatory with infection not excluded; however, both the second and third readers agreed that the study was positive for infection, and this interpretation was ultimately used.

Of the 25 included patients, 14 presented with one or more clinical sign or symptom of infection: 7 patients demonstrated fever, 8 patients demonstrated leukocytosis, 8 demonstrated positive driveline exit cultures (only performed on 20 patients), and 7 demonstrated positive blood cultures (only performed on 23 patients). Of these 14, all but one case were confirmed to have LVAD-specific infections. This patient presented with fever, leukocytosis, and positive blood culture, but was ultimately diagnosed with a nonVAD-related bacteremia. Additional patients included in this study had scans performed for oncological reasons, and incidentally had an LVAD.

A total of 19 patients were ultimately diagnosed with active LVAD-specific infection, comprised of 13 patients initially demonstrating symptoms and an additional 6 asymptomatic patients with known chronic LVAD infections on prophylactic antibiotics. All 19 patients with active LVAD-specific infection were correctly diagnosed on ^{18}F-FDG PET/CT. No false positive cases were identified.

Leukocytosis was evaluated in all patients. Of the 19 diagnosed with active LVAD-specific infection, only 8 demonstrated expected leukocytosis and 11 did not; however, an additional 8 of these 11 were on chronic antibiotic suppression and another 2 were placed on short term antibiotic suppression. This resulted in only a single patient diagnosed with active LVAD-specific infection not demonstrating expected leukocytosis and not on any antibiotic therapy. Of the 6 diagnosed without active LVAD-specific infection, 3 had leukocytosis but had comorbidities that would explain the results: 2 had known chronic non-LVAD infections, and the third had a healing sternotomy and was admitted for cardiac failure ultimately resulting in death.

Table 3. ^{18}F-FDG PET measurements of SUV$_{max}$ at each of the five LVAD locations calculated for patients with and without LVAD infections, as determined from the PET/CT images

| Location	Number of patients		Mean SUV$_{max}$ ± standard deviation		P-value	Best cutoff SUV$_{max}$
	No Infection	Infection	No Infection	Infection		
Driveline exit	18	7	2.5 ± 1.0	5.7 ± 2.3	< 0.01	3.8
Subcutaneous driveline	10	15	2.7 ± 0.5	7.1 ± 3.5	< 0.01	3.6
Pump	18	7	3.1 ± 0.9	8.1 ± 4.2	< 0.01	4.3
Inflow cannula	21	4	3.4 ± 0.8	7.0 ± 1.4	< 0.01	5.7
Outflow cannula	19	6	3.3 ± 1.0	7.3 ± 1.5	< 0.01	5.2
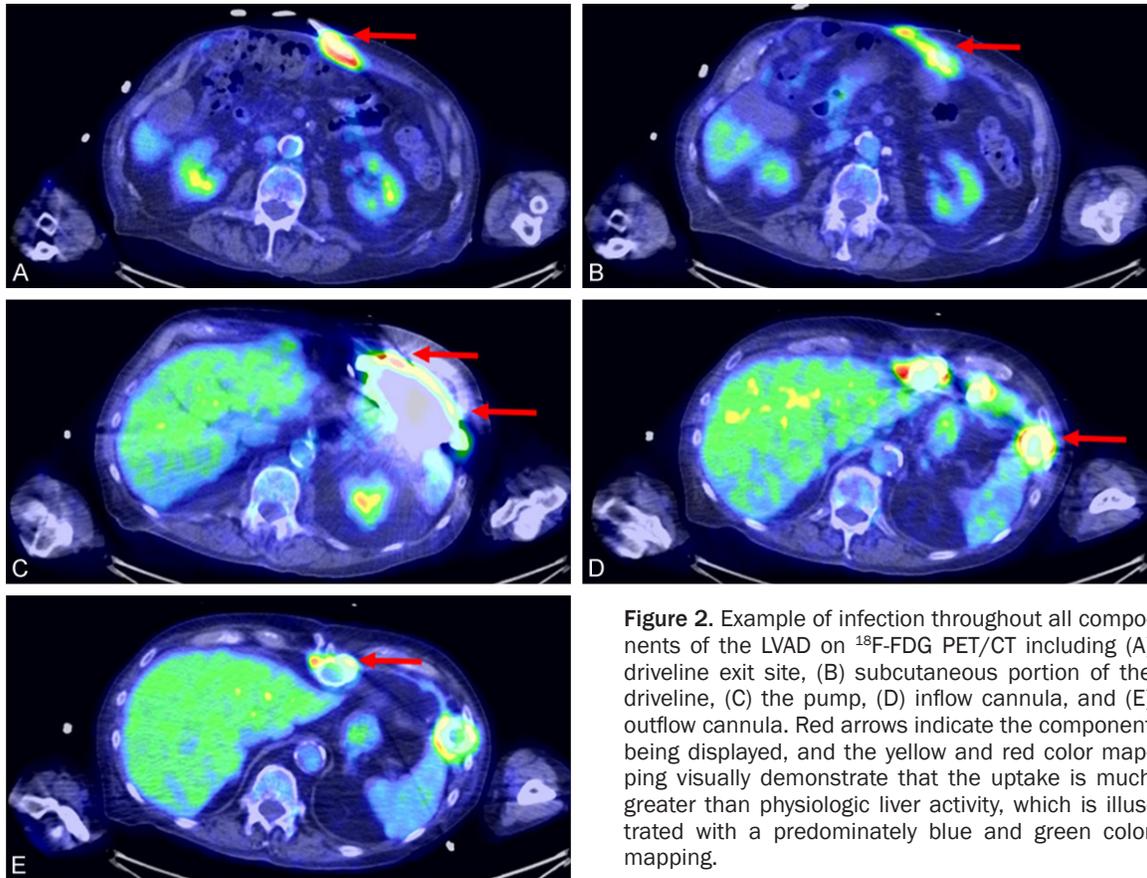
Figure 2. Example of infection throughout all components of the LVAD on ^{18}F-FDG PET/CT including (A) driveline exit site, (B) subcutaneous portion of the driveline, (C) the pump, (D) inflow cannula, and (E) outflow cannula. Red arrows indicate the component being displayed, and the yellow and red color mapping visually demonstrate that the uptake is much greater than physiologic liver activity, which is illustrated with a predominately blue and green color mapping.

C-reactive protein (CRP) evaluation was performed on 11 of the 25 patients: 8 diagnosed with and 3 diagnosed without LVAD-specific infection. Of the 8 diagnosed with LVAD-specific infection, only 1 had a negative CRP; however, he had a known chronic LVAD-specific infection and was receiving long-term IV antibiotics. The 3 patients without LVAD-specific infection but positive CRP results correspond to the same patients noted above demonstrating leukocytosis and comorbidities that could be the source of the results. The single patient diagnosed with active LVAD-specific infection but not demonstrating expected leukocytosis did not have CRP evaluation performed.

A comparison of SUV$_{max}$ for each of the five LVAD regions when LVAD-specific infection was absent and present as determined from the PET/CT images is summarized in **Table 3**. A significant difference between the two groups ($P < 0.01$) was calculated in all regions. Examples of positive infections at each LVAD region is illustrated in **Figure 2**. The mean SUV$_{max}$ range at noninfected sites was 2.5-3.4 and infected sites had a range of 5.7-8.1. Receiver
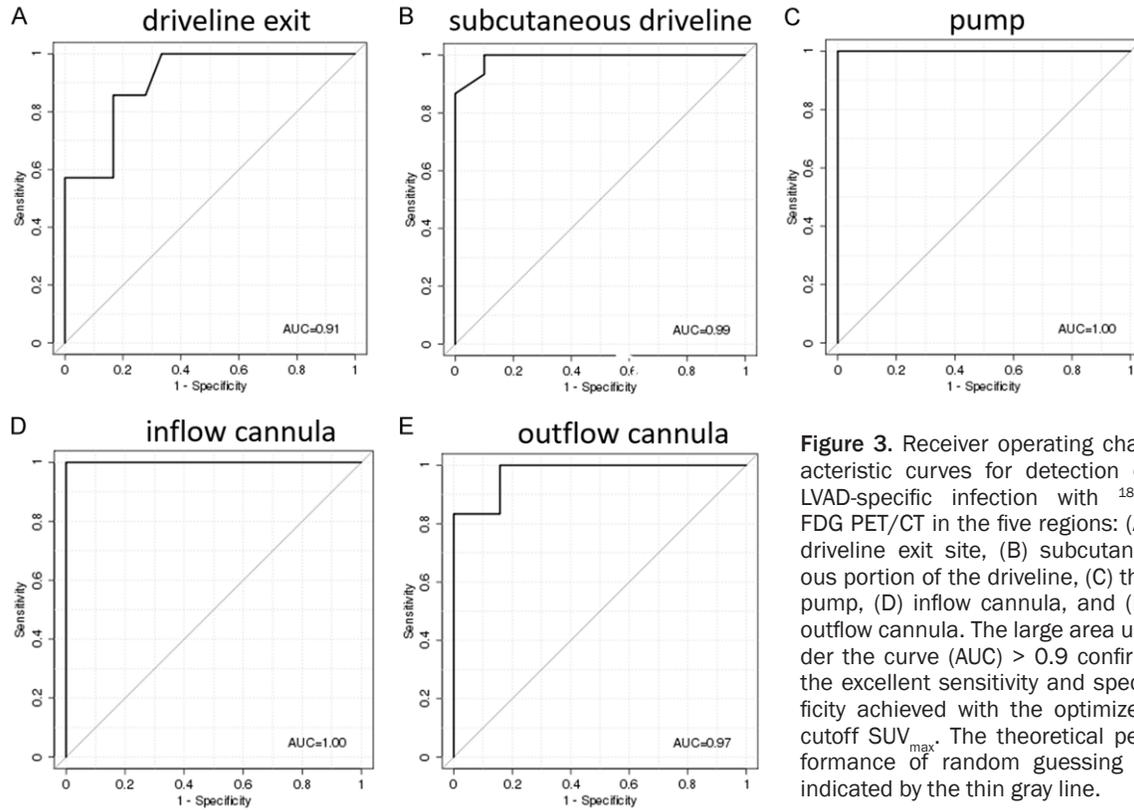
Figure 3. Receiver operating characteristic curves for detection of LVAD-specific infection with ^{18}F-FDG PET/CT in the five regions: (A) driveline exit site, (B) subcutaneous portion of the driveline, (C) the pump, (D) inflow cannula, and (E) outflow cannula. The large area under the curve (AUC) > 0.9 confirm the excellent sensitivity and specificity achieved with the optimized cutoff SUV_{max}. The theoretical performance of random guessing is indicated by the thin gray line.

Table 4. ^{18}F-FDG PET parameters calculated from volumes of hypermetabolic activity in the 19 positive cases for LVAD-specific infection: standardized uptake value mean and peak (SUV_{mean} and SUV_{peak}, respectively), metabolic tumor volume (MTV), and total lesion glycolysis (TLG)

Parameter	Mean ± standard deviation
SUV_{mean}	3.1 ± 0.8
SUV_{peak}	6.2 ± 2.4
MTV	190 ± 472
TLG	426 ± 768

operating characteristic (ROC) curves for each region are presented in **Figure 3**.

Calculated optimal site-specific cutoff SUV_{max} are listed in **Table 3** with a range of 3.6-5.7, and an overall cutoff of SUV_{max} of 5 is proposed. While this value is conservative for the driveline exit, subcutaneous, and pump regions, it is slightly below the cannulae site-specific values. However, only a single patient had an LVAD infection localizing only to the cannulae, with corresponding SUV_{max} 4.9, and this same patient was the previously-described one not exhibiting expected leukocytosis.

Additional quantitative measurements on the 19 patients with active LVAD-specific infections is summarized in **Table 4**. SUV_{mean} and SUV_{peak} followed similar trends to measured SUV_{max}, and may provide better measurements for noisy data. MTV and TLG had standard deviations greater than the calculated mean, and reflected poor surrogates for infection evaluation. This is due to the large range of hypermetabolic volumes and corresponding infection extents.

Chronic suppressive/prophylactic antibiotic treatment was given to 14 of the 19 patients diagnosed with LVAD-specific infections. In addition, 4 of the remaining 5 patients not on chronic treatment were given antibiotics prior to the PET study. This resulted in only a single patient diagnosed with an LVAD-specific infection receiving neither prophylactic nor treatment antibiotics.

Of the 19 patients diagnosed with LVAD-specific infections, 16 had either a positive driveline exit or blood culture. Two had negative driveline exit cultures, but did not have blood cultures performed. A single patient had no cultures performed. However, 3 patients diag-

Table 5. Results of cultures performed on driveline exit sites, blood, and post explantation LVADs

Organism	Driveline exit culture (N=13)	Blood culture (N=10)[3]	LVAD culture (N=4)
Staphylococcus aureus	6	3	3
Enterococcus	1	2	0
Coagulase negative Staphylococci	4	1	0
Streptococcus species	0	2	0
Candida	0	1	0
Corynebacterium species	0	1	0
Gram negative bacilli	1	1	1
Cutibacterium acnes	1	0	0

[3]N=10; however, one patient had 2 organisms, and thus 11 occurrences are listed.

nosed without an LVAD-specific infection also had positive driveline exit cultures and 2 had positive blood cultures. Details on identified organisms for positive cultures is summarized in **Table 5**. Details of the antibiotic treatment for the 19 patients diagnosed with LVAD-specific infections are presented in **Table 6**. Pictures of positive driveline infections are presented in **Figure 4**.

A total of 9 patients died during the study period, 6 of which were due to LVAD-specific or LVAD-related infections. The remaining 3 causes of death were: small cell lung cancer, intracranial hemorrhage due to pancytopenia (possibly related to nonLVAD-related candidemia), and sepsis due to a nonLVAD-related urinary tract infection.

A transesophageal echo (TEE) was performed on 10 of the 19 patients diagnosed with LVAD infection. TEE did not demonstrate signs of infection in all cases.

Discussion

In this study, we found ^{18}F-FDG PET/CT to be highly accurate for the diagnosis of LVAD-specific infection with a sensitivity of 100% and specificity of 100%. We recommend an overall cutoff SUV_{max} 5 to confirm LVAD infection. These findings support observations from earlier studies [10, 14, 16].

Infectious complications of MCSD therapy are the most common adverse event and are associated with increased healthcare expenditure and significantly reduced patient overall survival rates [6, 20, 21]. VAD-related and VAD-

specific infections can be challenging to diagnose, especially if involving deeper VAD regions. In addition, bloodstream infections are common in patients with MCSDs, the majority of which do not represent VAD-related infection [22]. Inability to accurately define these infectious syndromes may lead to unnecessary and expensive device explantation, or unnecessary antimicrobial therapy followed by chronic suppression. While ^{18}F-FDG PET/CT is not yet accredited for cardiac-related infection, and PET examinations for infection evaluation are often not covered by insurance, ^{18}F-FDG PET/CT has immense potential to improve the accuracy of MCSD infection to optimize patient care and potentially result in a net financial savings.

Approximately one third of the patients diagnosed with LVAD-specific infections in our study did not have any specific symptoms related to VAD infection. Even objective laboratory evaluations of leukocytosis and CRP provided false negative results in some patients ultimately diagnosed with infection. However, these patients were on chronic suppressive antibiotic therapy, and therefore paucity of clinical symptoms and even inaccurate laboratory results were not unexpected. Suppressive antibiotic therapy is frequently employed for patients with suspected VAD infections, and our results illustrate the importance of objective infection assessment through imaging and supportive laboratory results, independent of clinical presentation. Of note, many earlier studies evaluating use of ^{18}F-FDG PET/CT for VAD infection diagnosis did not report on ongoing antibiotic therapy prior to PET imaging [14, 16, 23]. Moreover, laboratory and clinical results can be confounding in the presence of nonVAD-related infections, as noted in two of our patients, as well as antibiotic treatment, and imaging may be required to isolate the infectious source; isolated laboratory evaluation is insufficient.

Our proposed overall cutoff SUV_{max} 5 would result in a false-negative in the patient with

Table 6. Summary of antibiotic treatment for the 19 patients diagnosed with LVAD infection

Number of patients on prophylactic antibiotics	Number of patients treated with antibiotics prior to PET study	Antibiotic treatment period prior to PET (mean days ± standard deviation)[4]	Range (days)[4]
14	16	21 ± 25	2-77

[4]N=13; insufficient information was present in the chart to calculated the value for 3 patients.
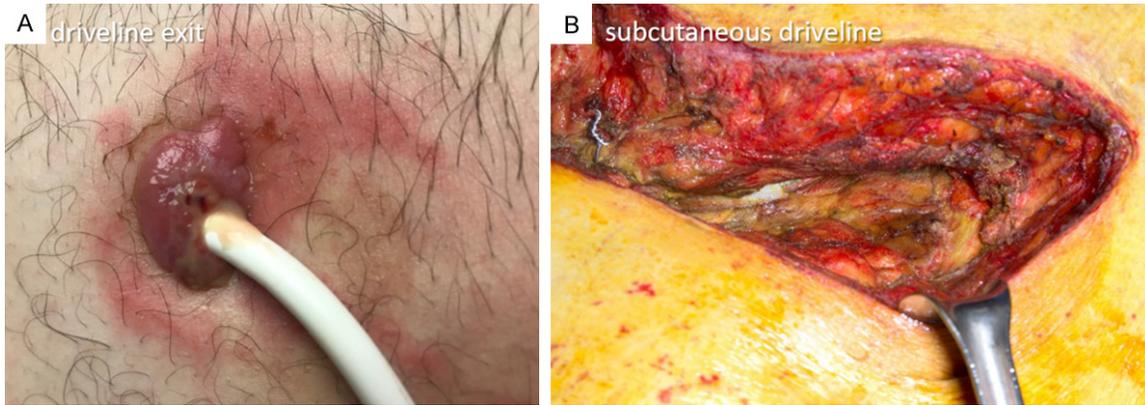
Figure 4. Example of (A) driveline exit site and (B) subcutaneous portion of the driveline infections. Note the erythema and purulent discharge.

LVAD infection localizing only to the cannulae and corresponding SUV_{max} 4.9 on imaging. The ultimate diagnosis was based on a combination of driveline exit site drainage with positive culture, and the suspicious FDG distribution on imaging. The lack of imaging findings of driveline exit site infection cannot be readily explained. Furthermore, it is this same patient that did not demonstrate expected leukocytosis. This patient may reflect a bad data point, and it is possible that the confusing findings are a result of incomplete records, such as the presence of chronic antibiotic suppression, or an ultimate misdiagnosis of infection, which would require misleading contaminated cultures. A measurement so close to the cut-off value would hopefully result in both the Nuclear Radiologist and clinical team evaluating the case in greater depth, going beyond an isolated measured SUV_{max} to form a final decision.

Alternative potential imaging modalities for diagnosing VAD infection have substantial limitations. MRI evaluation is generally precluded by the metallic LVAD hardware. Echocardiography, even transesophageal, may not be adequate for cardiac device related infectious endocarditis [24], and our study supports these observations.

CT imaging for attenuation correction is a standard part of most PET reconstruction algorithms, and co-registration is often essential for anatomical localization and accurate interpretation. While the sensitivity and specificity of isolated CT for VAD-specific infection are not well quantified, they are likely limited even with the aid of contrast and higher-dose diagnostic techniques. None of the identified LVAD infections from the current study could be confidently diagnosed from the accompanying CT data alone.

Most CT attenuation correction algorithms introduce artifacts in the presence of metal, such as the metallic driveline and pump, resulting in localized SUV inflation. Uncorrected reconstruction data can be compared to differentiate between true ^{18}F-FDG activity and artifact. Due to the retrospective nature of this study and lack of archived uncorrected data, a comparison could not be performed during the subsequent data review. This is expected to inflate our measured SUV_{max} at these locations. Access to non-attenuation-corrected reconstruction images, while recommended for accurate interpretation, is likely not critical based on our findings.

Additional potential limitations of ^{18}F-FDG PET/CT for VAD infection diagnosis include timing of imaging following implantation and physiologic myocardial FDG uptake. Visualization of infection on ^{18}F-FDG PET/CT performed shortly

after VAD implantation may be limited by postoperative inflammatory uptake. However, others have found ^{18}F-FDG PET/CT to be highly accurate for diagnosis of VAD infection even within 3 months of implantation [16]. Efforts to reduce physiologic myocardial uptake include use of a myocardial-suppressive low-carbohydrate/high-fat diet for 24 hours prior to the scan, fasting for at least 6 hours prior to the scan, and use of heparin bolus prior to imaging [10, 15, 25]. These measures switch the myocardial energy source from glucose to fatty acids and thus minimize any confounding myocardial ^{18}F-FDG uptake. While these measures are useful in ^{18}F-FDG PET/CT imaging for infective endocarditis and cardiac implantable electronic device infections [26], their utility in VAD infections remains unclear. Only 3 of the 25 included patients in this study had confirmed suppressive diets prior to imaging within their charts. Additional prospective studies with standardized preparatory protocols may be helpful in clarifying the utility of these measures for VAD infections.

Our study is retrospective with associated limitations. In particular, the lack of standardized indications, antibiotic therapy use prior to imaging, as well as lack of standardized imaging protocols including variable timing of PET/CT in imaging of possible VAD infection, inconsistent use of myocardial suppressive measures, use of different PET scanners, and use of different software and processing techniques all remain limitations. However, our results are congruent with earlier publications, suggesting these limitations are not critical, and the retrospective nature of the study enabled a larger sample size, improving the power of our study. As more patients receive VADs, and ^{18}F-FDG PET/CT VAD evaluation becomes more common, a shift to objective prospective studies will be facilitated.

The limited number of patients, not only in our study but other previously-published studies as well, necessitates additional retrospective and hopefully prospective studies. As more centers publish their data and analyses, parameters to diagnosis LVAD-specific infection can be confirmed and further refined.

Conclusion

^{18}F-FDG PET/CT is a useful adjunctive tool for assessment of LVAD infection and infection site localization, especially in the presence of confounding suppressive antibiotic therapy and nonVAD-related infections. We recommend a cut-off SUV$_{max}$ 5 to help diagnose infected LVAD sites.

Disclosure of conflict of interest

None.

Address correspondence to: Saul N Friedman, Division of Nuclear Medicine, Mallinckrodt Institute of Radiology, 510 South Kingshighway Boulevard, St. Louis, MO 63110, USA. Tel: 314-273-0989; E-mail: saul.friedman@gmail.com

References

[1] Benjamin EJ, Muntner P, Alonso A, Bittencourt MS, Callaway CW, Carson AP, Chamberlain AM, Chang AR, Cheng S, Das SR, Delling FN, Djousse L, Elkind MSV, Ferguson JF, Fornage M, Jordan LC, Khan SS, Kissela BM, Knutson KL, Kwan TW, Lackland DT, Lewis TT, Lichtman JH, Longenecker CT, Loop MS, Lutsey PL, Martin SS, Matsushita K, Moran AE, Mussolino ME, O'Flaherty M, Pandey A, Perak AM, Rosamond WD, Roth GA, Sampson UKA, Satou GM, Schroeder EB, Shah SH, Spartano NL, Stokes A, Tirschwell DL, Tsao CW, Turakhia MP, VanWagner LB, Wilkins JT, Wong SS and Virani SS; American Heart Association Council on Epidemiology and Prevention Statistics Committee and Stroke Statistics Subcommittee. Heart disease and stroke statistics-2019 update: a report from the American Heart Association. Circulation 2019; 139: e56-e528.

[2] Kirklin JK, Pagani FD, Kormos RL, Stevenson LW, Blume ED, Myers SL, Miller MA, Baldwin JT, Young JB and Naftel DC. Eighth annual INTERMACS report: special focus on framing the impact of adverse events. J Heart Lung Transplant 2017; 36: 1080-1086.

[3] Miller LW, Pagani FD, Russell SD, John R, Boyle AJ, Aaronson KD, Conte JV, Naka Y, Mancini D, Delgado RM, MacGillivray TE, Farrar DJ and Frazier OH; HeartMate II Clinical Investigators. Use of a continuous-flow device in patients awaiting heart transplantation. N Engl J Med 2007; 357: 885-896.

[4] Slaughter MS, Rogers JG, Milano CA, Russell SD, Conte JV, Feldman D, Sun B, Tatooles AJ, Delgado RM 3rd, Long JW, Wozniak TC, Ghumman W, Farrar DJ and Frazier OH; HeartMate II Investigators. Advanced heart failure treated with continuous-flow left ventricular assist device. N Engl J Med 2009; 361: 2241-2251.

[5] Gordon RJ, Weinberg AD, Pagani FD, Slaughter MS, Pappas PS, Naka Y, Goldstein DJ, Dem-

bitsky WP, Giacalone JC, Ferrante J, Ascheim DD, Moskowitz AJ, Rose EA, Gelijns AC and Lowy FD; Ventricular Assist Device Infection Study Group. Prospective, multicenter study of ventricular assist device infections. Circulation 2013; 127: 691-702.

[6] Hannan MM, Xie R, Cowger J, Schueler S, By T, Dipchand AI, Chu VH, Cantor RS, Koval CE, Krabatsch T, Hayward CS, Nakatani T and Kirklin JK. Epidemiology of infection in mechanical circulatory support: a global analysis from the ISHLT mechanically assisted circulatory support registry. J Heart Lung Transplant 2019; 38: 364-373.

[7] Litzler PY, Manrique A, Etienne M, Salles A, Edet-Sanson A, Vera P, Bessou JP and Hitzel A. Leukocyte SPECT/CT for detecting infection of left-ventricular-assist devices: preliminary results. J Nucl Med 2010; 51: 1044-1048.

[8] Bhargava P, He G, Samarghandi A and Delpassand ES. Pictorial review of SPECT/CT imaging applications in clinical nuclear medicine. Am J Nucl Med Mol Imaging 2012; 2: 221-231.

[9] Erba PA, Sollini M, Conti U, Bandera F, Tascini C, De Tommasi SM, Zucchelli G, Doria R, Menichetti F, Bongiorni MG, Lazzeri E and Mariani G. Radiolabeled WBC scintigraphy in the diagnostic workup of patients with suspected device-related infections. JACC Cardiovascular Imaging 2013; 6: 1075-1086.

[10] de Vaugelade C, Mesguich C, Nubret K, Camou F, Greib C, Dournes G, Debordeaux F, Hindie E, Barandon L and Tlili G. Infections in patients using ventricular-assist devices: comparison of the diagnostic performance of 18F-FDG PET/CT scan and leucocyte-labeled scintigraphy. J Nucl Cardiol 2019; 26: 42-55.

[11] Kung BT, Seraj SM, Zadeh MZ, Rojulpote C, Kothekar E, Ayubcha C, Ng KS, Ng KK, Au-Yong TK, Werner TJ, Zhuang H, Hunt SJ, Hess S and Alavi A. An update on the role of ^{18}F-FDG-PET/CT in major infectious and inflammatory diseases. Am J Nucl Med Mol Imaging 2019; 9: 255-273.

[12] Tlili G, Picard F, Pinaquy JB, Domingues-Dos-Santos P and Bordenave L. The usefulness of FDG PET/CT imaging in suspicion of LVAD infection. J Nucl Cardiol 2014; 21: 845-848.

[13] Dell'Aquila AM, Mastrobuoni S, Alles S, Wenning C, Henryk W, Schneider SR, Deschka H, Sindermann JR and Scherer M. Contributory role of fluorine 18-fluorodeoxyglucose positron emission tomography/computed tomography in the diagnosis and clinical management of infections in patients supported with a continuous-flow left ventricular assist device. Ann Thorac Surg 2016; 101: 87-94.

[14] Avramovic N, Dell'Aquila AM, Weckesser M, Milankovic D, Vrachimis A, Sindermann JR and Wenning C. Metabolic volume performs better than SUVmax in the detection of left ventricular assist device driveline infection. Eur J Nucl Med Mol Imaging 2017; 44: 1870-1877.

[15] Akin S, Muslem R, Constantinescu AA, Manintveld OC, Birim O, Brugts JJ, Maat APWM, Fröberg AC, Bogers AJJC and Caliskan K. 18F-FDG PET/CT in the diagnosis and management of continuous flow left ventricular assist device infections: a case series and review of the literature. ASAIO J 2018; 64: e11-e19.

[16] Dell'Aquila AM, Avramovic N, Mastrobuoni S, Motekallemi A, Wisniewski K, Scherer M, Sindermann JR and Wenning C. Fluorine-18 fluorodeoxyglucose positron emission tomography/computed tomography for improving diagnosis of infection in patients on CF-LVAD: longing for more 'insights'. Eur Heart J Cardiovasc Imaging 2018; 19: 532-543.

[17] Tam MC, Patel VN, Weinberg RL, Hulten EA, Aaronson KD, Pagani FD, Corbett JR and Murthy VL. Diagnostic accuracy of FDG PET/CT in suspected LVAD infections: a case series, systematic review, and meta-analysis. JACC Cardiovasc Imaging 2020; 13: 1191-1202.

[18] Kanapinn P, Burchert W, Körperich H and Körfer J. ^{18}F-FDG PET/CT-imaging of left ventricular assist device infection: a retrospective quantitative intrapatient analysis. J Nucl Cardiol 2019; 26: 1212-1221.

[19] Kendi AT, Magliocca K, Corey A, Nickleach DC, Galt J, Higgins K, Beitler JJ, El-Deiry MW, Wadsworth JT, Hudgins PA, Saba NF and Schuster DM. Do 18F-FDG PET/CT parameters in oropharyngeal and oral cavity squamous cell carcinomas indicate HPV status? Clin Nucl Med 2015; 40: e196-e200.

[20] Miller LW, Guglin M and Rogers J. Cost of ventricular assist devices: can we afford the progress? Circulation 2013; 127: 743-748.

[21] Shah N, Agarwal V, Patel N, Deshmukh A, Chothani A, Garg J, Badheka A, Martinez M, Islam N and Freudenberger R. National trends in utilization, mortality, complications, and cost of care after left ventricular assist device implantation from 2005 to 2011. Ann Thorac Surg 2016; 101: 1477-1484.

[22] Aslam S, Xie R, Cowger J, Kirklin JK, Chu VH, Schueler S, de By T, Gould K, Morrissey O, Lund LH, Martin S, Goldstein D and Hannan M. Bloodstream infections in mechanical circulatory support device recipients in the international society of heart and lung transplantation mechanically assisted circulation support registry: epidemiology, risk factors, and mortality. J Heart Lung Transplant 2018; 37: 1013-1020.

[23] Kim J, Feller ED, Chen W, Liang Y and Dilsizian V. FDG PET/CT for early detection and localization of left ventricular assist device infection:

impact on patient management and outcome. JACC Cardiovasc Imaging 2019; 12: 722-729.

[24] Habib G, Lancellotti P, Antunes MJ, Bongiorni MG, Casalta JP, Del Zotti F, Dulgheru R, El Khoury G, Erba AP, Iung B, Miro JM, Mulder BJ, Plonska-Gosciniak E, Price S, Roos-Hesselink J, Snygg-Martin U, Thuny F, Tornos Mas P, Vila-costa I and Zamorano JL; ESC Scientific Document Group. 2015 ESC Guidelines for the management of infective endocarditis: the Task Force for the Management of Infective Endocarditis of the European Society of Cardiology (ESC). Endorsed by: European Association for Cardio-Thoracic Surgery (EACTS), the European Association of Nuclear Medicine (EANM). Eur Heart J 2015; 36: 3075-3128.

[25] Scholtens AM, Verberne HJ, Budde RP and Lam MG. Additional heparin preadministration improves cardiac glucose metabolism suppression over low-carbohydrate diet alone in ^{18}F-FDG PET imaging. J Nucl Med 2016; 57: 568-573.

[26] Van Riet J, Hill EE, Gheysens O, Dymarkowski S, Herregods MC, Herijgers P, Peetermans WE and Mortelmans L. (18)F-FDG PET/CT for early detection of embolism and metastatic infection in patients with infective endocarditis. Eur J Nucl Med Mol Imaging 2010; 37: 1189-1197.